23rd ABCM International Congress of Mechanical Engineering
December 6-11, 2015, Rio de Janeiro, RJ, Brazil

CURVATURE EFFECTS OF VIBRATIONAL POWER FLOW THROUGH EULER-BERNOULLI BEAMS

Paulo Martins
Arcanjo Lenzi
Laboratório de Vibrações e Acústica - LVA, Universidade Federal de Santa Catarina - UFSC. Florianópolis-SC, Brazil.
paulo.victor@lva.ufsc.br and arcanjo@lva.ufsc.br

Abstract. *The scope of this project is to analyze curvature effects on vibrations, i.e. the vibrational power flow changes through a smooth bend in the plane of curvature. This phenomenon is particularly of interest since extensional and transversal waves are coupled. In addition, the parametrization of this phenomena is relatively complex due to the dependency on two non-related constants, i.e. the radius and bend angle. This paper starts with a brief literature review on the works of Walsh and White (2000), Wu and Lundberg (1996) and Kang* et al. *(2003). The (non-dimensional) parametrization differs in literature; this work therefore discusses a suitable set of non-dimensional parameters for algebraic simplifications. Thereafter, this paper presents the equations of motion of an Euler-Bernoulli's curved beam. Moreover, it analytically examines the coupling between extensional and transversal waves, and the differences of straight and curved wavenumbers. Finally, equations for transmission and reflection coefficients were derived with the wave propagation approach. The results depict the effects of curvature on transmission and reflection coefficients. Two cases were considered, e.g. deviating bend angles with constant radius, and varying radii with constant bend angle.*

Keywords: *curvature, wavenumber, powerflow, Euler-Bernoulli, propagation*

1. BASIC CONCEPTS OF CURVATURES

This work will focus on the investigation of vibrations only in the plane of curvature of a bent beam, whose geometric characteristics are constants in all its extent. The discontinuity introduces a peculiar complexity to the system since it couples the extensional and transversal displacements and the equations of motion becomes more sofisticated.

This section is based on works of Leissa and Qatu (2011), Walsh and White (2000), Wu and Lundberg (1996) and Kang *et al.* (2003), and will describe how to obtain the equations of motion for a curved beam based on Love's and Euler-Bernoulli's theories.

Walsh and White (2000) also derive equations for a curved beam considering Timoshenko's theory (which considers rotatory inertia and shear deformation) as well as Flügge's theory. However they won't be used in this paper, hence being omitted for simplicity's sake. The authors also derive equations for vibrational power flow within all cited theories.

Wu and Lundberg (1996) describe equations for transmission and reflection coefficients for a curvature's incident wave. They do an extensive analysis about their analytical results for 4 values of curvature parameter, 3 values of frequency each.

Kang *et al.* (2003) also analyze discontinuities effects in curved beams, deriving coefficient matrices for cases of kinetic discontinuities (changes in stiffness, mass and damping through beam's extent), curvature changes and special boundary conditions.

1.1 Equations of Motion

The central line of a curved beam is defined by the polar coordinate s (Fig. 1), where

$$s = R\theta, \tag{1}$$

which R represents the curvature radius between its center and its central line, and θ means the bend angle.

The central line deformation ϵ_0 and curvature change κ are given by

$$\epsilon_0 = \frac{\partial u}{\partial s} + \frac{v}{R}, \qquad \kappa = -\frac{\partial^2 v}{\partial s^2} + \frac{1}{R}\frac{\partial u}{\partial s}, \tag{2}$$

where u and v defines central line's displacements in s and z directions, respectively.

The extensional force N and moment M are results of axial tension integration over the beam's cross section, given by

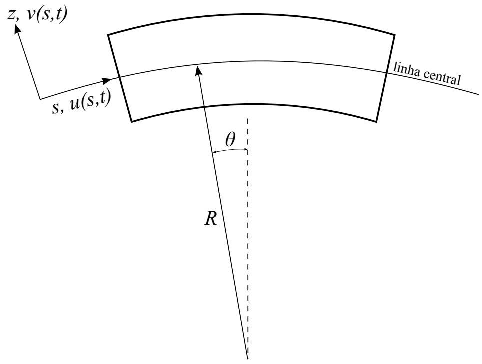

Figure 1. Geometric coordinates of a curved beam.

$$N = EA\epsilon_0, \qquad M = EI\kappa, \tag{3}$$

where E denotes the elasticity modulus of beam's material, A the cross-section's area and I the area's second moment of inertia. One assumes that these parameters are constants.

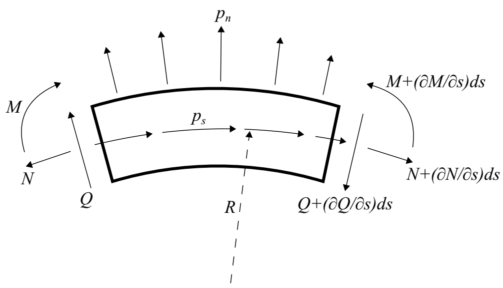

Figure 2. Infinitesimal curved beam element's schema.

By observing a beam's infinitesimal element (Fig. 2) it allows to balance the forces to obtain the equations of motion, without rotatory inertia nor shear deformation, as

$$\begin{bmatrix} \left(EA + \frac{EI}{R^2}\right)\frac{\partial^2}{\partial s^2} & \left(\frac{EA}{R} - \frac{EI}{R}\frac{\partial^2}{\partial s^2}\right)\frac{\partial}{\partial s} \\ sim. & EI\frac{\partial^4}{\partial s^4} + \frac{EA}{R^2} \end{bmatrix} \begin{Bmatrix} u \\ v \end{Bmatrix} + \begin{bmatrix} -\rho A & 0 \\ 0 & \rho A \end{bmatrix} \frac{\partial^2}{\partial t^2} \begin{Bmatrix} u \\ v \end{Bmatrix} = \begin{Bmatrix} -p_s \\ p_n \end{Bmatrix}. \tag{4}$$

One can see that both extensional and transversal motions are coupled within this governing equation's matrix form.

1.2 Curvature's Vibrational Analysis

The analysis of a curved beam's vibrational behaviour consists in considering harmonic displacements $u = Ue^{-i(ks+\omega t)}$ and $v = Ve^{-i(ks+\omega t)}$, where U and V represents extensional and transversal wave amplitudes, respectively; k the wavenumber (same value for both types of motion), ω defines the angular frequency, t the time and $i = \sqrt{-1}$. Also one assumes that body loads p_s and p_n are null, hence one can write Eq. 4 as

$$\begin{bmatrix} -\left(A + I/R^2\right)Ek^2 + \rho A\omega^2 & -\left(Ik^2 + A\right)iEk/R \\ sim. & \left(Ik^4 + A/R^2\right)E - \rho A\omega^2 \end{bmatrix} \begin{Bmatrix} U \\ V \end{Bmatrix} = 0, \tag{5}$$

which describes the curved beam's equation of motion for vibrational analysis.

Now, to write Eq. 5 in non-dimensional parameters is interesting because it focus on simplicity without losing information about curvature characteristics. The parameters were chosen with intent of considering curve's radius, geometrical properties and beam's material. The parametrization used by Walsh and White (2000) and Kang *et al.* (2003) is introduced on the following

$$\gamma = Rk, \quad \Omega = \frac{\omega R^2}{r_g c_e}, \quad K^2 = \frac{r_g^2}{R^2}, \tag{6}$$

with $r_g = \sqrt{I/A}$ and $c_e = \sqrt{E/\rho}$, where γ and Ω means the non-dimensional wavenumber and frequency, and K represents the curvature parameter based on gyration radius. Wu and Lundberg (1996) uses a slightly different with $\gamma = kr_g$ and $\Omega = r_g/c_e$, but these won't be used in this work.

Special attention must be given to the curvature characteristic K. In case of the cross-section to have dimensions close to the curvature radius R, the equation of motion in Eq. 5 loses physical meaning by not considering shear deformation nor rotatory inertia. For example, there is a maximum value of $K = 0.25$ for a circular cross-section because this implies that its curvature radius R is equals to cross-section's radius.

By substituting Eq. 6 in 5 gives

$$\begin{bmatrix} -\gamma^2 + K^2\left(\Omega^2 - \gamma^2\right) & i\gamma(1+\gamma^2K^2) \\ sim. & 1 + K^2\left(\gamma^4 - \Omega^2\right) \end{bmatrix} \begin{Bmatrix} U \\ V \end{Bmatrix} = 0. \tag{7}$$

Since there's coupling between movements, one can write the displacement ration U/V in two ways

$$\beta_u = \frac{U}{V} = \frac{i\gamma\left(K^2\gamma^2+1\right)}{-\gamma^2 + K^2\left(\Omega^2-\gamma^2\right)}, \qquad \beta_v = \frac{V}{U} = \frac{i\gamma\left(K^2\gamma^2+1\right)}{1 + K^2\left(\gamma^4-\Omega^2\right)}. \tag{8}$$

By doing the determinant of Eq. 7 equal to 0, one obtains a characteristic equation of wavenumber, as

$$\gamma^6 - \left(2 + K^2\Omega^2\right)\gamma^4 + \left\{1 - \left(1+K^2\right)\Omega^2\right\}\gamma^2 + K^2\Omega^4 - \Omega^2 = 0. \tag{9}$$

So one can observe that, in γ^2, the equation above have three pairs of complex conjugate numbers as solutions, which are the curved structure's wavenumbers. Therefore the wavenumbers γ can be addressed as γ_j for $j = 1, 2, 3$, knowing that $\gamma_{4,5,6} = -\gamma_{1,2,3}$. Hence, the relations described on Eq. 8 can be updated to

$$\beta_{uj} = \frac{i\gamma_j\left(K^2\gamma_j^2+1\right)}{-\gamma_j^2 + K^2\left(\Omega^2-\gamma_j^2\right)}, \qquad \beta_{vj} = \frac{i\gamma_j\left(K^2\gamma_j^2+1\right)}{1 + K^2\left(\gamma_j^4-\Omega^2\right)}. \tag{10}$$

The real and imaginary parts of γ_j are represented in Fig. 3. As the γ_j are functions of frequency Ω and of curvature parameter K, the value of $K = 0.025$ for a rectangular cross-section obtaining the illustrated curves.

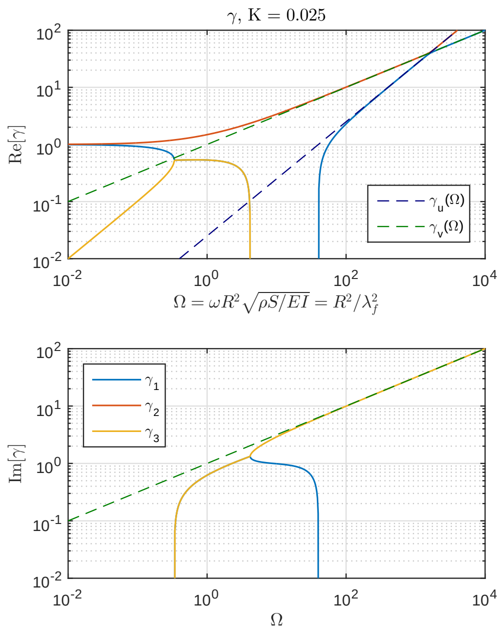

Figure 3. Variation of wavenumbers γ_j with non-dimensional frequency Ω for the curvature parameter $K = 0,025$.

Figure 3 allows a better overview of structure's vibrational behaviour through a closer observation of its wavenumbers. It is known that for real values of γ_j, one have a wave in the form $e^{\pm i\gamma_j\theta}$, i.e., it represents a propagating wave. For imaginary γ_j one have $e^{\pm\gamma_j\theta}$, or it has only decaying waves that can be neglected depending on beam's length. Finally, complex γ_j gives both propagating and evanescent parts. Applying these concepts, Fig. 3 shows 4 regions:

Region I All $\gamma_{1,2,3}$ have real values, i.e. all waves are in propagation, without attenuation. According to Lee *et al.* (2007), each mode j is responsible for carrying energy alone.

Region II Only γ_2 is real while the others are complex and equal in modulus, indicating the appearance of a decaying part in two modes. For that, γ_2 still carrying energy independently while modes 1 and 3 needs to interact with each other in order to produce a path for allowing energy to flow.

Region III Now γ_{1and3} becomes purely imaginary indicating that, for the energy to flow in these 2 modes the positive-going and negative-going waves of same type must interact, i.e. γ_1-γ_4 and γ_3-γ_6.

Region IV Here γ_1 becomes real and approximates from γ_u, which is the non-dimensional extensional wavenumber for a straight beam. Also can be observed that γ_3 approximates from $i\gamma_2$, and they both approaches in module from γ_v. The later characterizes the non-dimensional transversal wavenumber for a straight beam. This shows that, in this region, a soft bend starts to behave as the same way as a straight beam, i.e. the waves don't undergo the curvature's distinct effects.

Knowing the 3 pairs of wavenumbers and since the displacements are coupled, by applying the displacement ratios of Eq. 10, one may write solutions for Eq. 7 as

$$\begin{Bmatrix} u(\theta,t) \\ v(\theta,t) \end{Bmatrix} = \begin{bmatrix} U_1^+ & \beta_{u2}V_2^+ & \beta_{u3}V_3^+ & U_1^- & -\beta_{u2}V_2^- & -\beta_{u3}V_3^- \\ \beta_{v1}U_1^+ & V_2^+ & V_3^+ & -\beta_{v1}U_1^- & V_2^- & V_3^- \end{bmatrix} \begin{Bmatrix} e^{-i\gamma_1\theta} \\ e^{-i\gamma_2\theta} \\ e^{-i\gamma_3\theta} \\ e^{+i\gamma_1\theta} \\ e^{+i\gamma_2\theta} \\ e^{+i\gamma_3\theta} \end{Bmatrix} e^{-i\omega t}, \tag{11}$$

which is very important to solve problems that depends on analytical approaches, as long as they reduce by half the number of constants to be determined in the curvature. Can be noted as well that, for the negative-going waves, the values for β_{v1}, β_{u2} and β_{u3} are negative too since $\gamma_{4,5,6} = -\gamma_{1,2,3}$.

Another observation to be made on Eq. 9, as well as on Fig. 3, is to do $\gamma \to 0$, giving

$$\lim_{\gamma\to 0} (9) = \left(K^2\Omega^2 - 1\right)\Omega^2 = 0. \tag{12}$$

The solution for above's equation gives 4 roots, being two in $\Omega_{1,2} = 0$, one in $\Omega_3 = -1/K$ which don't have physical meaning, and $\Omega_4 = \Omega_c = 1/K$. This Ω_c can be found on literature as the ring frequency, and means that the predominantly extensional wave of the beam have a length equals to the curvature radius R.

Other important observation to be made on Fig. 3 is that $\gamma_1 \to \gamma_u$ and $\gamma_2, |\gamma_3| \to \gamma_v$, which are the extensional and transversal wavenumbers of a straight beam, respectively. These wavenumbers already are in non-dimensional form given by $\gamma_u = Rk_u$ and $\gamma_v = Rk_v$, being $k_u = \omega\sqrt{\rho/E}$ and $k_v = \sqrt[4]{\omega^2\rho A/EI}$ so $\gamma_u = \Omega K$ and $\gamma_v = \sqrt{\Omega}$. Those values can also be obtained by simply doing $K \to 0$ (i.e., $R \to \infty$) in Eq. 9.

2. ENERGY TRANSMISSION AND REFLECTION COEFFICIENTS

For calculating the coefficents, one may consider a curved beam connecting two semi-infinity straight beams, with one propagating wave hitting the bend. While this occurs, the curvature responds by vibrating and part of the wave is reflected and part is transmitted. No losses were considered, as Fig. 4 depicts.

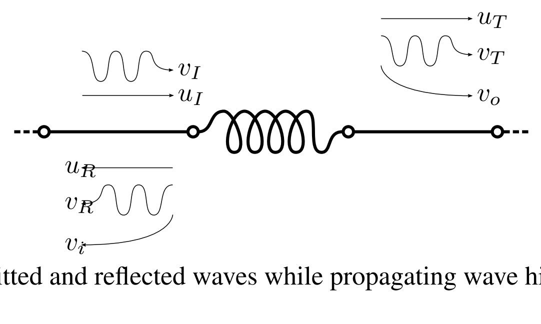

Figure 4. Transmitted and reflected waves while propagating wave hits a descontinuity

This setup provided a suitable model for better understanding what the curvature effects under a vibrational point of view. The focus was to analyze how angle and radius can change wave propagation, and to do this all other influencing aspects were neglected.

For considering anechoic boundaries, a major difficulty of this work was to implement the special semi-infinite element in commercial softwares, e.g. ANSYS and Comsol. The formulation for this type of element was given by Gavric (1992) as

$$\left[\tilde{K}_{si}\right] = \begin{bmatrix} ik_u EA & 0 & 0 \\ 0 & (i-1)k_v^3 EI & ik_v^2 EI \\ 0 & ik_v^2 EI & (i+1)k_v EI \end{bmatrix} \tag{13}$$

and it shows that transversal and rotation movements are coupled, as result of flexural waves. This implementation was prohibitive because softwares didn't have a direct access to build custom elements, and they couldn't handle the coupling at the time. So, a FEM algorithm was built to comprise these boundary conditions.

MATLAB was used to produce this framework, implementing 1D Euler-Bernoulli beam elements from Zienkiewicz and Taylor (2005) and Cook *et al.* (2007). The elements have 2 nodes, 3 degrees of freedom each (translations on x and y directions and rotation in ψ), as one can see on Fig. 5.

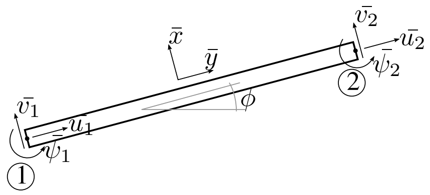

Figure 5. Beam element used to discretize the geometry on the custom FEM algorithm.

The force applied was also specific through it had to simulate a positive-going wave coming from the infinity. Thus, it was also obtained from Gavric (1992) as

$$F_{in} = -2 \begin{Bmatrix} ik_u EAu_\infty \\ (1-i)k_v^3 EIv_\infty \\ (i-1)k_v^2 EIv_\infty \end{Bmatrix}. \tag{14}$$

2.1 Displacement Functions' Constants Obtainment

With the FEM framework working properly, one needs to obtain the displacement function's constant that will be used to calculate the power coefficients. Accordingly, the next equations of displacement are considered

$$\begin{aligned} u_e &= u_I e^{-ik_u x} + u_R e^{+ik_u x}, \\ v_e &= v_I e^{-ik_v x} + v_R e^{+ik_v x} + v_i e^{+k_v x} \end{aligned} \tag{15}$$

for waves acting before the discontinuity and

$$\begin{aligned} u_s &= u_T e^{-ik_u x}, \\ v_s &= v_T e^{-ik_v x} + v_o e^{-k_v x}, \end{aligned} \tag{16}$$

for the transmitted waves after the curve. One notices that the inciding wave have no evanescent part, and there's no counter-reflection by the boundary conditions. Hence, in order to determine u_I, v_I, u_R, v_R, v_i, u_T, v_T and v_o, one may simply pick the FEM's displacement results from the straight part of the mesh to compose a system of equations, e.g.

$$\begin{bmatrix} e^{-ik_u x_1} & e^{+ik_u x_1} & 0 & 0 & 0 \\ e^{-ik_u x_2} & e^{+ik_u x_2} & 0 & 0 & 0 \\ 0 & 0 & e^{-ik_v x_1} & e^{+ik_v x_1} & e^{+k_v x_1} \\ 0 & 0 & e^{-ik_v x_2} & e^{+ik_v x_2} & e^{+k_v x_2} \\ 0 & 0 & e^{-ik_v x_3} & e^{+ik_v x_3} & e^{+k_v x_3} \end{bmatrix} \begin{Bmatrix} u_I \\ u_R \\ v_I \\ v_R \\ v_i \end{Bmatrix} = \begin{Bmatrix} u_{FEM}(x_1) \\ u_{FEM}(x_2) \\ v_{FEM}(x_1) \\ v_{FEM}(x_2) \\ v_{FEM}(x_3) \end{Bmatrix}, \tag{17}$$

for the section before the curvature, and

$$\begin{bmatrix} e^{-ik_u x_4} & 0 & 0 \\ 0 & e^{-ik_v x_4} & e^{-k_v x_4} \\ 0 & e^{-ik_v x_5} & e^{-k_v x_5} \end{bmatrix} \begin{Bmatrix} u_T \\ v_T \\ v_o \end{Bmatrix} = \begin{Bmatrix} u_{FEM}(x_4) \\ v_{FEM}(x_4) \\ v_{FEM}(x_5) \end{Bmatrix} \tag{18}$$

for the segment after the curvature, being x_1, x_2 and x_3 nodes on input, and x_4 and x_5 nodes on the output.

After solving the system of equations, i.e. with the constants properly calculated, one may consider a time-average power by doing

$$P = -\frac{1}{T}\int_0^T F\frac{\partial x}{\partial t}dt, \tag{19}$$

where P is the power, T the period, F a generic force and x the displacement on same force's direction.

For an extensional power, one may write

$$\begin{aligned} P_e &= -\frac{1}{T}\int_0^T \left[N\frac{\partial u}{\partial t}\right] dt \\ &= -\frac{\omega}{2\pi}\int_0^{2\pi/\omega} \left[\left(-iEAk_uUe^{i(k_ux-\omega t)}\right)\left(-i\omega Ue^{i(k_ux-\omega t)}\right)\right] dt, \end{aligned} \tag{20}$$

that by solving above's equation

$$P_e = \frac{1}{2}EA\omega k_u\tilde{u}^2. \tag{21}$$

Using the standard non-dimensional quantities introduced before, the equation above can be rewritten as

$$P_e = \frac{1}{2}EAc_e\frac{\Omega^2K^2}{R^2}\tilde{u}^2, \tag{22}$$

remembering that $c_e = \sqrt{E/\rho}$, R representing the curvature radius and $\tilde{u}$ serve as a extensional displacement's constant.

Analogously, one may write the flexural power as

$$P_f = EI\frac{\Omega^{5/2}K}{R^4}c_e\tilde{v}^2, \tag{23}$$

where $\tilde{v}$ means a transversal displacement's constant.

By knowing this, one may divide transmitted and reflected by the incident powers to obtain the coefficients. So, the following

$$\begin{cases} R_{ef} = \dfrac{P_e^R}{P_e^I} = \dfrac{u_R^2}{v_I^2}, \\ R_{ff} = \dfrac{P_f^R}{P_e^I} = 2K\sqrt{\Omega}\dfrac{v_R^2}{v_I^2}, \end{cases} \qquad \begin{cases} T_{ef} = \dfrac{P_e^T}{P_e^I} = \dfrac{u_T^2}{v_I^2}, \\ T_{ff} = \dfrac{P_f^T}{P_e^I} = 2K\sqrt{\Omega}\dfrac{v_T^2}{v_I^2}, \end{cases} \tag{24}$$

gives the power coefficients for a flexural input wave. Coefficients for an extensional input won't be evaluated in this work, but they are well known and can be found on works of Wu and Lundberg (1996), Walsh and White (2000) and Lee *et al.* (2007).

3. RESULTS AND DISCUSSIONS

This section will focus only on flexural input because of its slightly higher complexity than extensional (shear and moment), but still allowing good observation of curvature peculiarities. Figures already have non-dimensional frequency transformed to Hertz.

Accordingly, one may observe in Fig. 6 that from 1 mm to 30 mm radius there's considerable changes on the transmission and reflection coefficients. Firstly the 1 mm plots shows a very symmetric aspect, typical from a sharp bend. On the other hand, for 30 mm radius there's several important changes on regions of 90° to 135° and 270°, and also for frequencies above 10^3 Hz when the wavelength is small and the wave starts to ignore the curvature (i.e. flexural transmission coefficient grows).

For 130°, at Fig. 7, one observes that flexural transmission coefficients makes a small slope for higher frequencies, while greater radii shows higher coeffients and small radii (below 5 mm) shows a decrease in transmission. This decrease

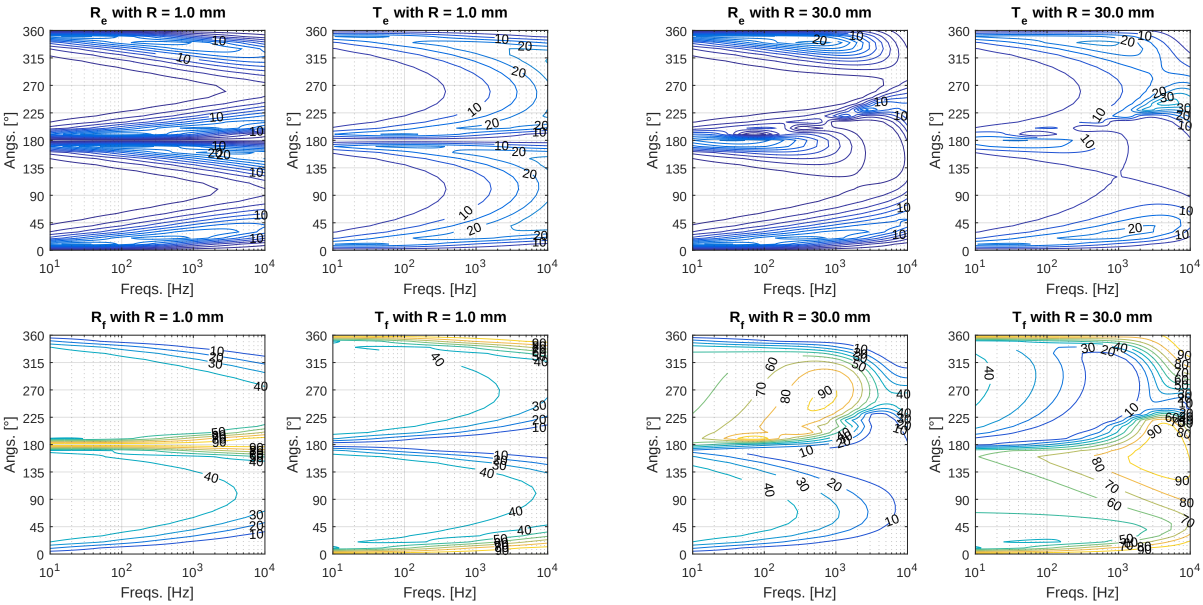

Figure 6. Power coefficients for unit flexural input in function of frequency [Hz] and bending angle θ, for a radius R of 1 mm and 30 mm.

is followed by an increase in extensional reflections and transmissions since the bottom-right corner depicts an increase of 20%. Therefore one may say that small radii and high frequencies enhances flexural-to-extensional shifts, as well as large radii with high frequencies enhances flexural transmission. Remembering that previous analysis are for a flexural incident wave.

In 180°, the figure depicts a peculiar region where, for a sharp bend it almost reflects all flexural wave, but as radius grows, reflection decreases. The graph also shows a well behaved region for "extensional shifting", where both flexural reflection and transmission are small and radius increases. Finally, for 270° is where major differences for sharp and smooth bends occurs. Also one can note that this bending angle reflects almost all flexural transmission, mostly while radius' increasing. Another interesting observation is that, for this angle, higher frequencies ultimately influence the extensional transmission, i.e. incident flexural wave turn into extensional output waves.

4. REMARKS

This work explained basic concepts of curvatures, presenting formulations for equations of motion and discussed the wavenumbers of a curvature. Also presented an systematic approach for obtaining power coefficients for transmission and reflection waves. Was shown results for flexural incident waves with respect to frequency, bending angle and bending radii.

Analysis shown that sharp bends are symmetric with respect to bending angle, differing from smooth bending. In this case was used a radius of 30 mm and different regions were observed. At 180°, small radii will enhance flexural reflections. For larger radii, this region depicts a shift between high and low flexural transmission.

Was noted that the region of 130° shows a shift from flexural to extensional waves for sharp bends at high frequencies. Finally, 270° shows the major differences between sharp and smooth bends while flexural reflection increases with respect to radius within some point, but a flexural to extensional shift occurs for majority of tested radii, for high frequencies (close to 10^4 Hz).

5. REFERENCES

Cook, R.D., Malkus, D.S., Plesha, M.E. and Witt, R.J., 2007. *Concepts and applications of finite element analysis*. John Wiley & Sons, 4th edition.

Gavric, L., 1992. "Power-flow analysis using infinite beam elements". *Le Journal de Physique IV*, Vol. 2, No. C1, pp. C1–511.

Kang, B., Riedel, C. and Tan, C., 2003. "Free vibration analysis of planar curved beams by wave propagation". *Journal of Sound and Vibration*, Vol. 260, No. 1, pp. 19–44.

Lee, S.K., Mace, B.R. and Brennan, M.J., 2007. "Wave propagation, reflection and transmission in curved beams". *Journal of Sound and Vibration*, Vol. 306, pp. 636–656.

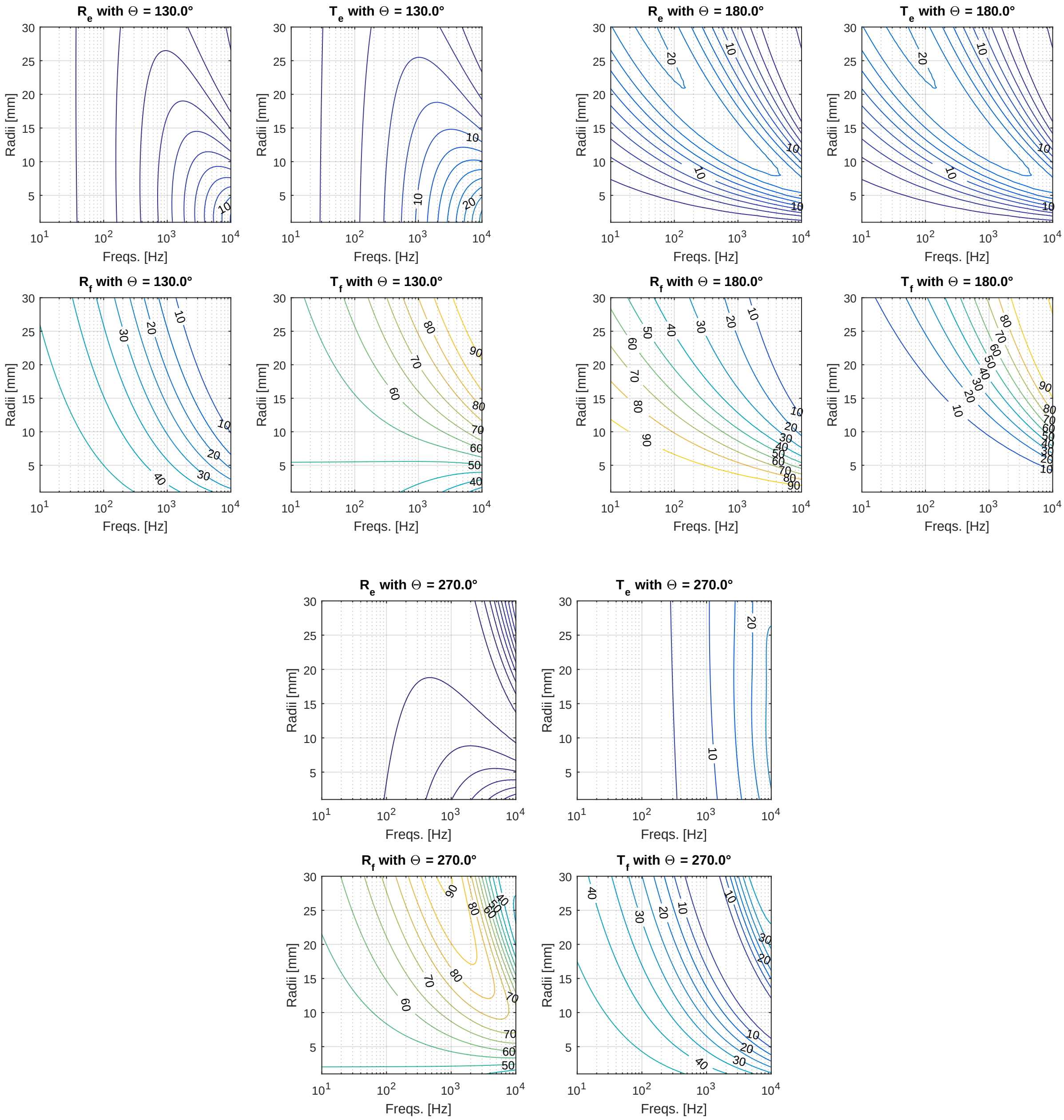

Figure 7. Power coefficients for unit flexural input in function of frequency [Hz] and radii R, for a bending angle θ of 130°, 180° and 270°.

Leissa, A. and Qatu, M., 2011. *Vibrations of Continuous Systems*. McGraw-Hill Education. ISBN 9780071714808. URL `http://books.google.com.br/books?id=59R1oLzNvCQC`.

Walsh, S.J. and White, R., 2000. "Vibrational power transmission in curved beams". *Journal of Sound and Vibration*, Vol. 233, No. 3, pp. 455–488.

Wu, C. and Lundberg, B., 1996. "Reflection and transmission of the energy of harmonic elastic waves in a bent bar". *Journal of Sound and Vibration*, Vol. 190, No. 4, pp. 645–659.

Zienkiewicz, O.C. and Taylor, R.L., 2005. *The finite element method for solid and structural mechanics*. Butterworth-heinemann, 6th edition.

6. RESPONSIBILITY NOTICE

The authors are the only responsible for the printed material included in this paper.